A Comparison of Large Eddy Simulations of Wind and Ocean Turbines

Ryan King and Spencer Alexander

December 13th, 2012

1   Introduction

High fidelity modeling of fluid flow is crucial in calculating mechanical loads, power production, and wake behaviors of wind and ocean turbines. The wind industry has suffered from unexpected gearbox failures and underperformance, and recent publications attribute these effects to poor characterization and prediction of the turbulent flow fields experienced by wind turbines. To alleviate these effects, CFD calculations must be able to model realistic atmospheric and ocean boundary layers flows that occur in wind and ocean turbine installations. In particular, these CFD simulations must account for turbulent coherent structures that are the primary cause of fatigue damage to wind turbine blades and drivetrains[KJS+05, LCM+11]. Additionally, these CFD simulations must include thermal stability effects because stability has been shown to impact the power production of single turbines and affect the wake behavior from arrays of turbines[WL12, WL11]. More accurate modeling of these turbulent flow fields will lead to improved wind turbine reliability and more energetic wind farm arrays, ultimately lowering the cost of renewable energy.

In response to these concerns, there have been several new developments in computational modeling of wind farms. In particular, large eddy simulations (LES) have been used to model wind turbines and their arrays in realistic ABL flows[CMM10, LPA11, ?, WPA10, SPK11]. In this study we take an LES approach to generating realistic neutrally stable and convective ABL's, and extend that framework to a stable ocean boundary layer (OBL). This approach builds on the Simulator for Offshore Wind Farm Applications (SOWFA) toolset developed by Matt Churchfield and Sang Lee at the National Wind Technology Center[SOW12]. This toolset uses OpenFOAM, an open source finite volume CFD program[Ope12], to generate precursor boundary layer simulations exhibiting realistic turbulent structures. Actuator line models of wind and ocean turbines are then inserted into the fully developed boundary layer flows following the work of Churchield and Troldborg[CLM+12, CLMM12, TSM07]. Our results show interesting differences in the wake behaviors of ocean and atmospheric turbines that have important implications for array optimization. Additionally, we discuss the emergence of numerical artifacts and comment on their impact on the choice of LES grid cell size.

2 Methodology

2.1 Physics

LES

In this study, we employ a Large Eddy Simulation (LES) to model the fluid flow in the atmospheric and ocean boundary layers. In an LES simulation a low pass spatial filter is applied to the incompressible Navier-Stokes equations so that the scales of turbulence responsible for transport and production of turbulent kinetic energy (TKE) are directly resolved, but smaller scales where viscous dissipation takes place are parameterized in a subfilter scale model (SFS) [Moe84]. The governing equations for our simulation include the Boussinesq approximation for buoyancy effects, Coriolis forces for a latitude of 45 deg north, and density-normalized forces representing our turbine actuator model. The governing equations by the filtered continuity equation,

$$\frac{\partial \bar{u}_j}{\partial x_j} = 0, \tag{1}$$

and the filtered momentum equation,

$$\frac{\partial \bar{u}_i}{\partial t} + \frac{\partial}{\partial x_j} \left(\bar{u}_j \bar{u}_i \right) = -\frac{\partial \tilde{p}}{\partial x_i} - \frac{\partial \tau_{ij}^D}{\partial x_j} + F_i^T + F_i^A, \tag{2}$$

where

$$\tilde{p} = \frac{\bar{p} + \tau_{kk}}{3\rho}. \tag{3}$$

The SFS model used to parameterize viscous effects and is the standard Smagorinsky model. This SFS model accounts for shear stress everywhere except at the lower boundary where a wall model is used. The SFS model is applied at cell faces, which avoids interpolating to cell faces while taking the divergence of stress but provides a less dissipative effect near the lower boundary surface. To model this, the shear stress equation is set to

$$\tau_{ij}^D = -2\nu^{SFS} \bar{S}_{ij}, \tag{4}$$

where

$$\bar{S}_{ij} = \frac{1}{2} \left(\frac{\partial \bar{u}_i}{\partial x_j} + \frac{\partial \bar{u}_j}{\partial x_i} \right). \tag{5}$$

The smagorinsky model defines ν as

$$\nu^{SFS} = (C_s \Delta)^2 (2\bar{S}_{ij}\bar{S}_{ij})^{1/2} \tag{6}$$

where C_s is the model constant set to 0.125 (check this for wind) and Δ is the filter length scale, which for SOWFA is set as $(\Delta x \Delta y \Delta z)^{1/3}$ Spatial filter Boussinesq approximation

Because of the sharp velocity gradients, complex surface roughness effects, and vortical structures that exist near the lower wall boundary, a wall model is applied at the lower

boundary instead of directly resolving the flow with a no-slip condition. This wall model accounts for the momentum and heat flux at the wall. In this study we apply the wall model of Moeng 1984, which estimates a friction velocity based on supplied roughness heights and surface temperature flux using the Monin-Obukhov similarity theory. This friction velocity then leads to the horizontally averaged shear stresses on the lower surface. The relevant equations are as follows:

Turbine Properties

The turbines modeled in our two simulation were not modeled as physical blades to which the fluid provided with rotational energy – the computation power and modeling difficulty of such blades are beyond the scope of this paper. Instead, the turbines were modeled as a set of actuator lines which impose body forces on the incoming fluid flow. This model is described by Sorensen and Shen [SS02] and implimented in SOWFA [SOW12].

For the onshore wind turbine simulations we used the "NREL Offshore 5-MW Baseline Wind Turbine[JBMS09], which is a representative utility scale multimegawatt wind turbine developed at NREL's National Wind Technology Center. It is based on the REpower 5M wind turbine, with additional data from other publicly available sources so that the structural, aerodynamic, material, and control system properties are representative of a modern day wind turbine. The wind turbine is three-bladed, upwind, variable speed, pitch controlled turbine with a 126 m rotor diameter, 90 m hub height, and high speed multi-stage gearbox. Rated power for the turbine is 5.0 MW at 12.1 rpm. Mass, stiffness, damping, and airfoil properties are given in NREL documentation[JBMS09].

For the ocean current turbine simulation, a 1MW turbine was modeled (hereafter refered to as the OT1MW), with specs based upon the Voith 1 MW [Voi12]. The OT1MW was modeled with a 8 meter blade radius and 1.5m hub. The airfoils used on the OT1MW were a scaled down version of the airfoils used on the NREL5MW turbine as found in the SOWFA package [SOW12], which is a poor approximation to the Voith 1MW turbine; future work will include a better representation of the 1MW turbine blade and generator properties. The OT1MW produced as expected, with the turbine reaching a steady state production of 0.85MW and steady rotation rate of 8 RPM at hub-height channel velocity of 1.9 m/s.

2.2   Numerics

The numerical package used in the simulations was OpenFOAM (Open Source Field Operation and Manipulation), which is a collection of C++ libraries for solving PDE's on unstructured meshes using the finite volume method [Ope12]. OpenFOAM is increasingly becoming the CFD package of choice for wind turbine simulations thanks to it?s open source and adaptable nature that has led to work done at the National Wind Technology Center and the University of Massachusetts Amherst [].

We employ the ABLPisoSolver developed as part of the NREL SOWFA (Simulator for Offshore Wind Farm Applications) toolset [SOW12] to solve our flow simulations. ABLPiso-Solver is based on the standard PISO algorithm that solves the momentum and pressure equations implicitly, but with the buoyancy, SFS stress, and (Coriolis, temperature, need to check the actual code on these as pdfs from Matt disagree) terms treated explicitly. These

explicit terms are solved sequentially using a Predictor-Corrector approach based on the previous timestep.

2.3 Simulation

Mesh

The atmospheric boundary layer precursor simulation was performed on a domain of 3000 m in the x-direction, 3000 m in the y-direction, and 1000 m in the z direction. The mesh for the precursor simulation was composed of 75x75x25 grid cells, giving a 40m resolution in each direction. The mesh was then decomposed into 6 smaller domains for parallel processing in MPI (Message Passing Interface) using a Scotch decomposition method. Finally, each decomposed domain was refined by a factor of two in all three coordinate directions, increasing the total number of cells eightfold to 1125000. Additionally, the grid was refined three times around the actuator turbine during the actuator simulations. As discussed later, this grid refinement leads to artifacts in the results

For the ocean current turbine simulation, the precursor domain size was 200 meters in the x-direction, 200 meters in the y-direction and 70 meters in the z-direction. The initial mesh in the precursor was set at 45x45x20 and was refined once. Each cell in the precursor measured approximately 4x4x3 meters. Future work will study the impact of domain cell resolution in the precursor step.

Domain size assumptions Grid cell size justification and differences between wind and water

Flow Conditions

Initial Conditions - ABL/OBL precursor simulation To generate realistic turbulent structures, we took the approach of running a precursor simulation that allowed atmospheric or ocean boundary layers to fully develop. Once the boundary layer was fully developed, we then inserted actuator line turbines into the simulation. The initial conditions for the atmospheric simulations were a uniform geostrophic wind velocity from $225°$ at $9m/s$, with perturbations added near the surface to cause the turbulent flow field to quickly develop. The ABL properties were specified such that the velocity at 90 m would be $9m/s$ and the driving pressure gradient was adjusted to maintain that velocity. The aerodynamic surface roughness Z_0 was 0.016. The temperature profile was constant at 300 K up to 750 m height where the temperature then increased to 308 K. This creates a capping inversion that defines the boundary layer and slows the vertical growth of the boundary layer that has been a problem in previous simulations. Surface temperature flux was set to 0 in the neutral ABL case and 0.04 mK/s in the unstable ABL case. Spencer to add ocean precursor IC's Maybe a quick image of the initial condition velocity/temp field?

The boundary conditions during the ABL precursor simulation on the top of the domain were: temperature gradient equal to that of the initial capping inversion, normal velocity and parallel velocity gradient equal to zero, the normal pressure gradient from the momentum equation, and zero gradient of SFS viscosity. On the bottom: prescribed temp flux, the normal pressure gradient from momentum equation, and normal velocity equal to zero,
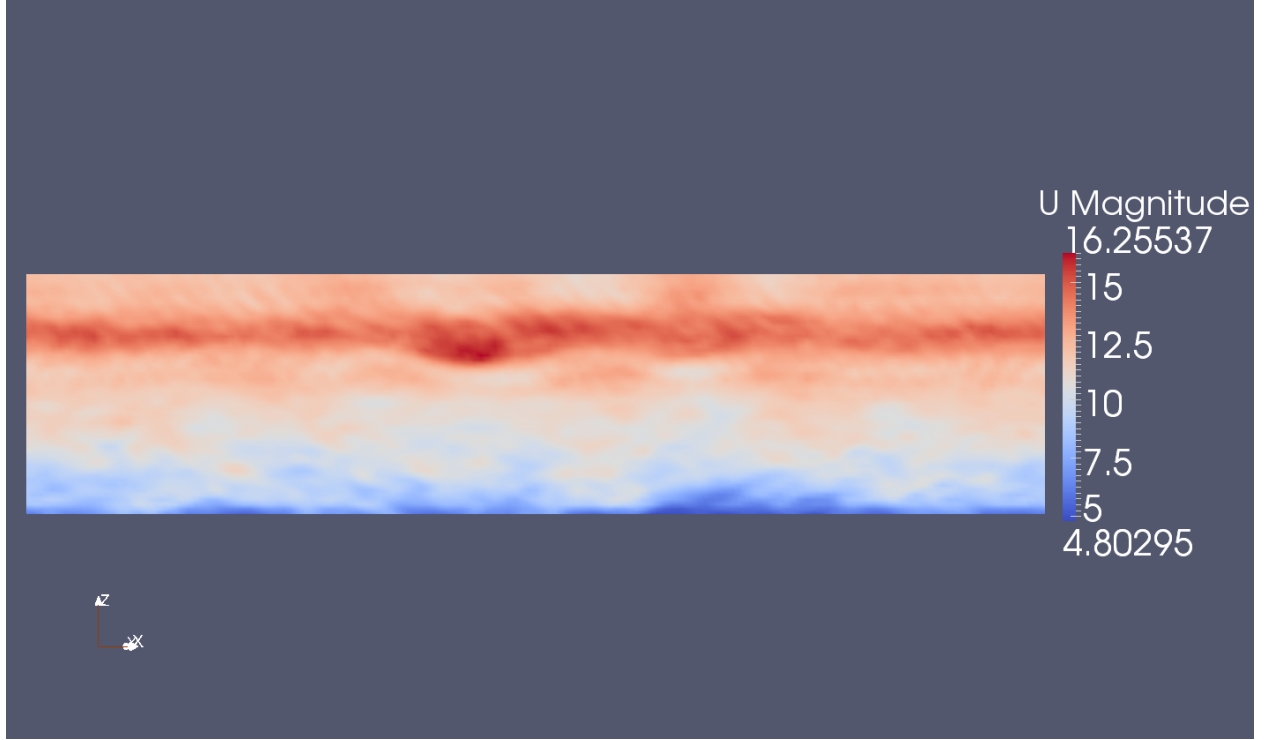
Figure 1: Precursor flow for the neutral ABL case

horizontal velocity from wall model (nonzero because OpenFOAM is a colocated code). Lateral walls used periodic boundary conditions to generate turbulent structures, and small perturbations were introduced on the bottom of the domain to accelerate their development.

The fully developed precursor simulation was run for an additional 2000 seconds, and slices of inflow data were saved at 0.5 second intervals to be used as boundary conditions in the actuator simulations.

3   Results

3.1   Precursor Results

After 12000 seconds of simulation time, the ABL precursor simulation showed fully developed atmospheric boundary layers. The temperature profile of the precursor ABL simulation shows the capping inversion that limits boundary layer growth and vertical motion above 750 m. Figures 1 show the fully developed flow fields for neutral and unstable ABL's after they've been allowed to spin up for 12000 seconds.

The OBL Precursor was run to 6000 seconds, which represents seven large-eddy turnovers [CLM+12]. At this point, the pressure gradient drove our velocity at 35 meters to 1.9 m/s and 2.2 m/s. The vertical velocity profile for the flow is shown in Figure 2.

The precursor simulations show realistic coherent turbulent structures that are crucial in generating realistic load distributions. The different stability cases also exhibit realistic vertical mixing and shear profiles, with the unstable case showing a better mixed boundary
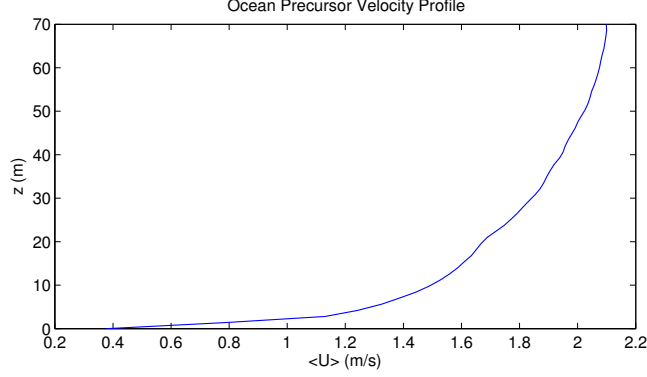
Figure 2: Vertical velocity profile for the OBL

layer.

3.2 Actuator Line Results

After fully developing the atmospheric boundary layer in the absence of wind turbines, we insert a single actuator line turbine and run the simulation for another 250 seconds. The results lead to several interesting insights. First, there is nontrivial flow leakage at the root of the blades that persists for about two rotor diameters downstream. This region where the blade airfoil properties are still discernible is the "near-wake" region[SPK11]. Further downstream in the "far-wake" region the blade-specific effects have diffused into an amorphous wake, but the velocity deficit that is characteristic of the far-wake is present for eight to ten rotor diameters. Figures XX show average velocity profiles and Figures XX show instantaneous velocity profiles at 250 seconds. The instantaneous velocities also show horizontal and vertical meandering of the wake that is likely caused by instabilities in the boundary layer.

Numerical Artifacts

Interestingly, we also observe numerical artifacts in the CFD results located at the transition between grid refinement regions. Figure 3 shows the average velocity at hub height for the unstable ABL with the actual grid cells overlaid on the flow field. Clearly, the artifacts are generated at the abrupt transition between adjacent refinement levels. Confirming these results, the ocean turbine simulation, where the grid refinement was constant across the entire domain, did not show any signs of artifacts – this is shown in Figure 4. However, a single grid refinement level is not the ideal solution – conversations with the SOWFA creators, Matt Churchfield and Sang Lee, suggest that a spatial filter or mesh smoothing function could help alleviate these anomalies.

Vertical wake oscillation

One very notable feature of the ocean current turbine flow was the extent to which vertical flow oscillation dominated the velocity profile. Figure 5 shows the movement of the vertical
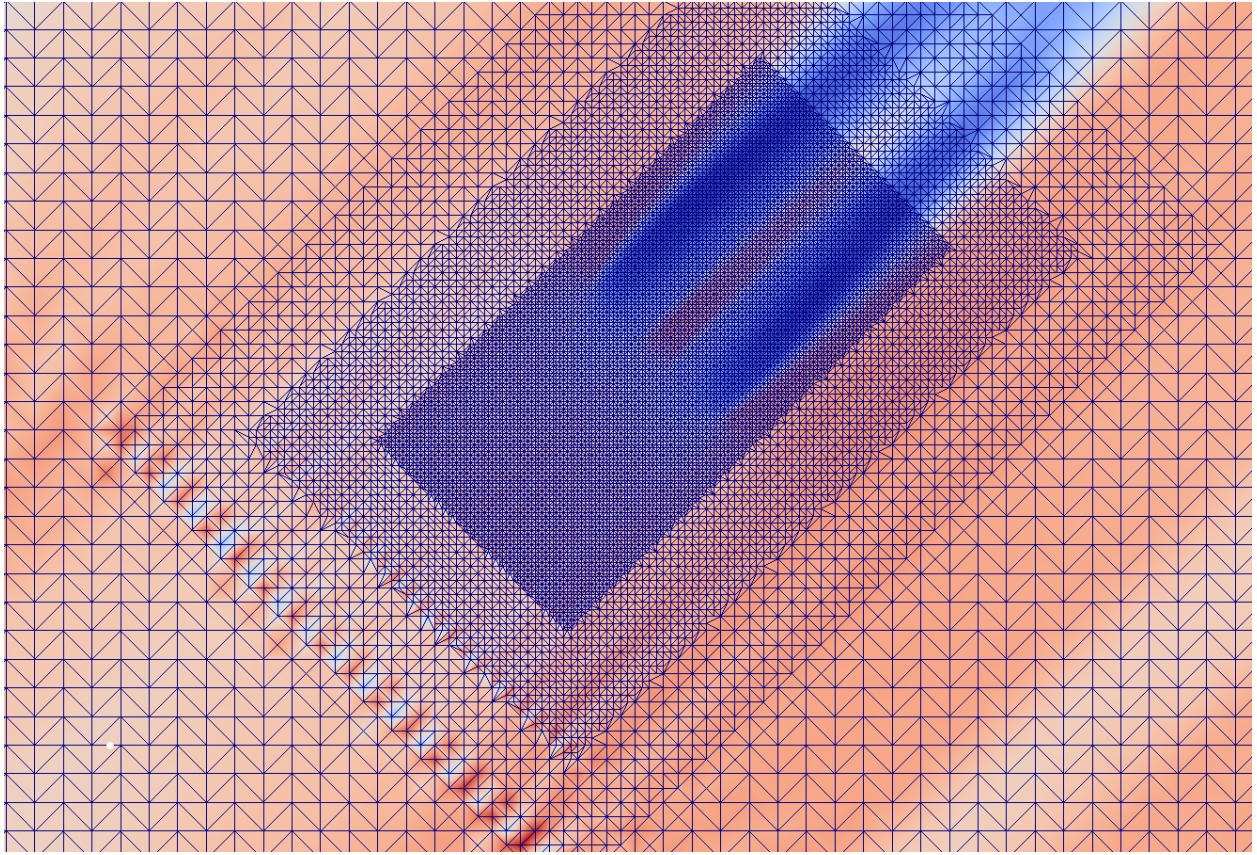
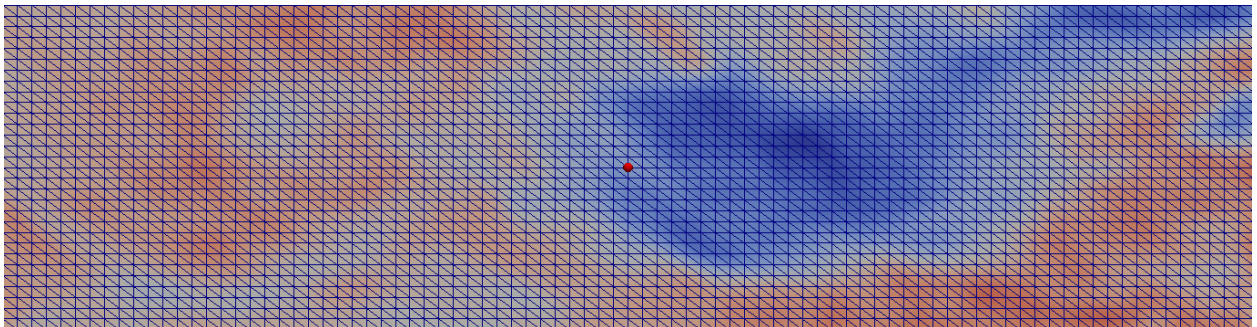Figure 3: Numerical artifacts present in the ABL wind turbine simulation

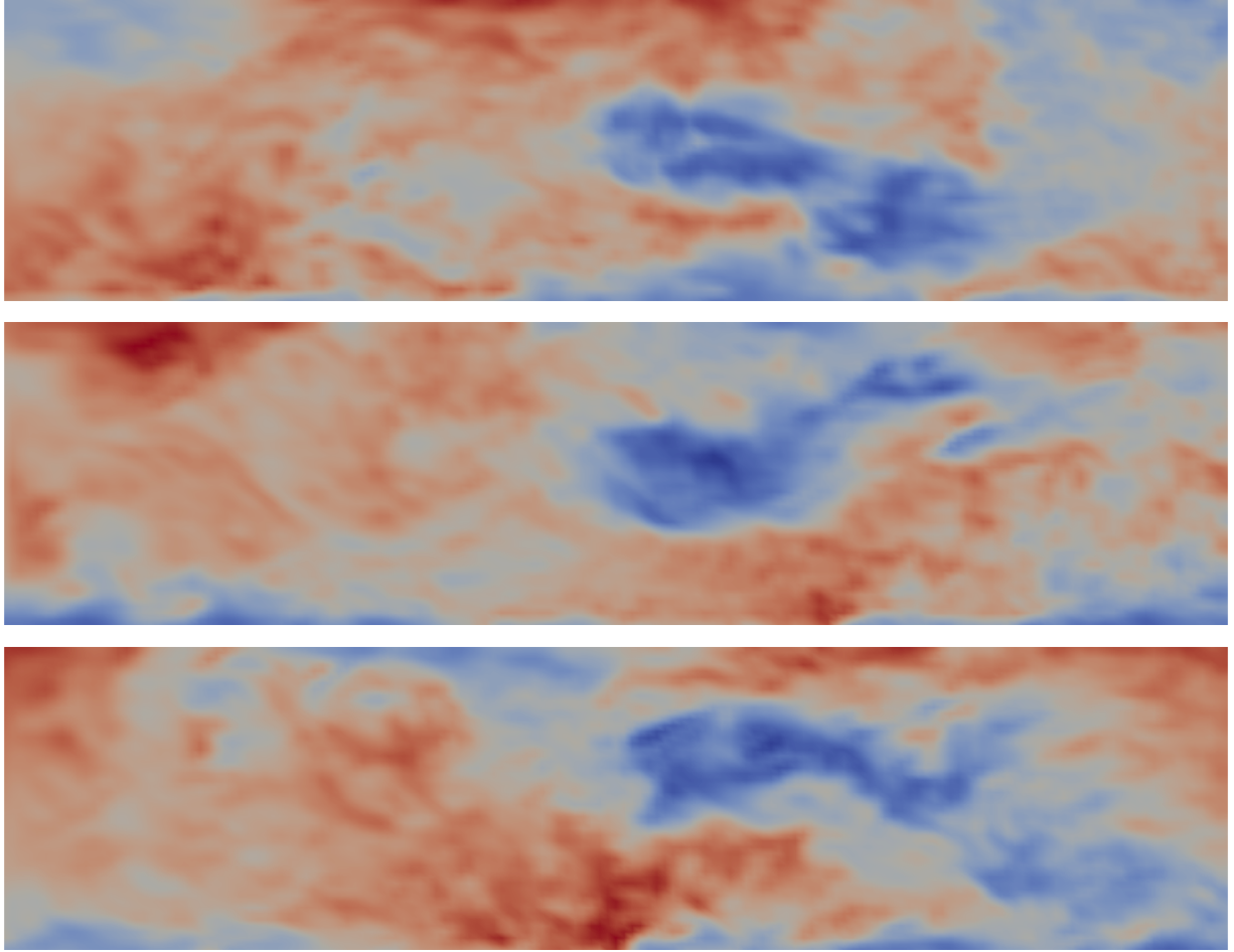Figure 4: Ocean wind turbine simulation without artifacts

Figure 5: Ocean turbine flow snapshots at t = 100s, 200s and 300s

oscillation, with three snapshots from 100, 200 and 300 seconds. While vertical oscillations were certainly noted in the wind energy simulation, the extent of the ocean turbine oscillatiosn is comparatively much greater, with the peaks of the oscillation covering most all of the 70 meter vertical domain.

4   Conclusion and Future Work

Future work ideas Aeroelastic modelling (FAST) Arrays of WTG?s Applications to control schemes, forecasting, array optimization

This work used standard numerical methods typical to CFD simulations, but opportunities exist to study the performance of other numerical methods. With the simplicity of the domain, the tendency towards smooth functions and the periodic boundary condition, spectral methods and wavelet decompositions would likely result in a substantial performance gain. Additionally, our simulations used the backward Euler method for time steps, where a performance would likely be gained in using the Crank Nicholson or Runge Kutta methods.

Future work on this project related to ocean turbine modeling includes several possibilities. For one, the grid size used in the initial model was very coarse, with a grid cell size of $2m^3$ in the precursor stage and $0.2m^3$ in the turbine modeling stage. A more accurate representation of the precursor flow could be obtained by doubling or tripping the resolution. Second, work remains on better modeling the various tidal turbines currently being proposed by the private sector; the model used in this paper was adapted from a wind turbine design. And finally, work remains in modeling various ocean states, such as stable, unstable, high wind shear/turbulence, etc.

References

[CLM+12] M. J Churchfield, S. Lee, P. J Moriarty, L. A Martinez, S. Leonardi, G. Vijayakumar, and J. G Brasseur. A large-eddy simulation of wind-plant aerodynamics: Preprint. January 2012.

[CLMM12] Matthew J. Churchfield, Sang Lee, John Michalakes, and Patrick J. Moriarty. A numerical study of the effects of atmospheric and wake turbulence on wind turbine dynamics. *Journal of Turbulence*, page N14, 2012.

[CMM10] Marc Calaf, Charles Meneveau, and Johan Meyers. Large eddy simulation study of fully developed wind-turbine array boundary layers. *Physics of Fluids*, 22:015110–015110–16, January 2010.

[JBMS09] J. Jonkman, S. Butterfield, W. Musial, and G. Scott. Definition of a 5-MW reference wind turbine for offshore system development. Technical report, February 2009.

[KJS+05] N. D Kelley, B. J Jonkman, G. N Scott, J. T Bialasiewicz, and L. S Redmond. Impact of coherent turbulence on wind turbine aeroelastic response and its simulation: Preprint. August 2005.

[LCM+11] S. Lee, M. Churchfield, P. Moriarty, J. Jonkman, and J. Michalakes. Atmospheric and wake turbulence impacts on wind turbine fatigue loading: Preprint. December 2011.

[LPA11] Hao Lu and Fernando PortÃ©-Agel. Large-eddy simulation of a very large wind farm in a stable atmospheric boundary layer. *Physics of Fluids*, 23(6):065101, 2011.

[Moe84] Chin-Hoh Moeng. A large-eddy-simulation model for the study of planetary boundary-layer turbulence. *Journal of the Atmospheric Sciences*, 41(13):2052–2062, July 1984.

[Ope12] Openfoam - the open source computational fluid dynamics (cfd) toolbox, December 2012.

[SOW12] Sowfa - simulator for offshore wind farm applications, December 2012.

[SPK11] B. Sanderse, S.P. Pijl, and B. Koren. Review of computational fluid dynamics for wind turbine wake aerodynamics. *Wind Energy*, 14(7):799–819, October 2011.

[SS02] Jens Norkaer Sorensen and Wen Zhong Shen. Numerical modeling of wind turbine wakes. *Journal of Fluids Engineering*, 124(2):393–399, 2002.

[TSM07] Niels Troldborg, Jens N SÃ¸rensen, and Robert Mikkelsen. Actuator line simulation of wake of wind turbine operating in turbulent inflow. *Journal of Physics: Conference Series*, 75:012063, July 2007.

[Voi12] Voith - tidal current power stations, December 2012.

[WL11] Sonia Wharton and Julie K Lundquist. Assessing atmospheric stability and its impacts on rotordisk wind characteristics at an onshore wind farm. *Wind Energy*, July 2011.

[WL12] Sonia Wharton and Julie K Lundquist. Atmospheric stability affects wind turbine power collection. *Environmental Research Letters*, 7(1):014005, March 2012.

[WPA10] Yu-Ting Wu and Fernando PortÃ©-Agel. Large-eddy simulation of wind-turbine wakes: Evaluation of turbine parametrisations. *Boundary-Layer Meteorology*, 138(3):345–366, December 2010.